Quasi-Superlattice Storage

A Concept of Multilevel Charge Storage

T.-C. Chang,[a,d,z] S. T. Yan,[b] P. T. Liu,[c,e] C. W. Chen,[b] H. H. Wu,[a] and S. M. Sze[b,c]

[a]*Department of Physics and Institute of Electro-Optical Engineering* [d]*Center for Nanoscience and Nanotechnology, National Sun Yat-sen University, Kaohsiung, 804 Taiwan*
[b]*Institute of Electronics,* [e]*Department of Photonics and Display Institute, National Chiao Tung University, Hsin-Chu, Taiwan* [c]*National Nano Device Laboratory, Hsin-Chu 300, Taiwan*

In this work, a novel concept of quasi-superlattice storage (QS^2) is demonstrated. Under a suitable operating voltage, two apparent states of charge storage can be distinguished. The memory effects are due to the multilevel charge storage within the quasi-superlattice. The multilevel charge storage provides a feasible design for the 2-bit-per-cell nonvolatile memory devices. Also, the leakage behavior of the quasi-superlattice structure has also been characterized by current-voltage measurements at room temperature and low temperatures. The resonant tunneling-like leakage characteristic is observed at low temperatures. A concise physical model is proposed to characterize the leakage mechanism of tunneling for the quasi-superlattice structure, and this suggests that consideration of the operating voltage for the 2-bit-per-cell nonvolatile memory device needs to be taken into account.

© 2004 The Electrochemical Society. [DOI: 10.1149/1.1808634] All rights reserved.

Recently, portable electronic devices, such as digital cameras, laptops, smart cards, mp3 players, USB FLASH, have received much attention in the market place and have significantly impacted the semiconductor industries. All the above mentioned products are based on the device of FLASH nonvolatile memory. The commercially available FLASH memory contains the structure of a poly-Si floating gate (FG), which serves as a charge-trapping layer.[1] Since the difficulties of consecutive scaling have been addressed,[2] the candidate, silicon-oxide-nitride-silicon (SONOS) nonvolatile memory device, is now in the position to become an important part of the industry.[3-6] SONOS possesses a structure similar to the FG memory device but silicon nitride rather than poly-Si is adopted as the charge-trapping layer.[7,8] The SONOS structure has a great potential of scaling the thickness of the tunnel oxide down to 1.6 nm and reducing the programming voltage below 5 V.[7,9] That, hence, improves the speed of performance of the memory device.[10] In this study, both Si and silicon nitride are utilized as the charge-trapping layers and a Si/silicon nitride quasi-superlattice structure is proposed as the multilevel charge storage for the first time. A 2-bit per cell Fowler-Nordheim (F-N) tunneling operation has been proposed for the electrical measurements. The leakage behavior of the quasi-superlattice stack for the multilevel charge storage has also been demonstrated and a concise model is proposed to derive and explain the leakage behavior of the quasi-superlattice gate stack.

Experimental

Single-crystal, 6 in. diam, (100) oriented p-type silicon wafers were used in the present study. The wafers were chemically cleaned by a standard RCA cleaning, followed by a dry oxidation in an atmospheric pressure chemical vapor deposition (APCVD) furnace at 925°C to form a 3 nm tunnel oxide. Subsequently, silicon nitride (Si_3N_4) and amorphous Si (a-Si) quasi-superlattice of two periods were deposited by low pressure chemical vapor deposition (LPCVD) at 780 and 550°C, respectively. Each of the four LPCVD layers was controlled to be about 2 nm. A 10 nm thick tetraethyl-orthosilicate (TEOS) oxide was deposited on the QS^2 as the control oxide layer. To densify the control oxide layer, a steam densification was performed at 982°C.[6,10] Via the TEOS oxide deposition and steam densification, the two a-Si layers were crystallized into microcrystals or polycrystals, which depends on the grain size of the Si layers. After the Al electrodes were patterned and sintered,

capacitance-voltage (C-V) measurements were performed to investigate the memory effects of the quasi-superlattice storage (QS^2) memory device.

Results and Discussion

Figure 1 shows the device structure in this work. The quasi-superlattice of Si_3N_4 and a-Si, sandwiched between the tunnel oxide and the control oxide, is utilized as a charge storage element for a memory device instead of poly-Si FG or Si_3N_4 single layer. Figure 2 shows the ideal energy band diagram of the QS^2 memory device at $V = 0$. The quasi-superlattice of Si_3N_4 and a-Si clearly shows the band offsets that can easily trap electrons as the storage elements. The undoped a-Si layers are with a wider bandgap than that of the Si substrate. To write the memory device, a positive gate voltage has to be applied to make electrons directly tunnel through the tunnel oxide by F-N tunneling. The tunneling electrons may be trapped in the trap states of the nitride layers, the interface states between Si_3N_4 and a-Si layers, or the quantum wells of the a-Si layers. The trapped electrons cause a threshold voltage shift (ΔV_t), memory window, of the memory device, which can be defined as 1 or 0, according to the different threshold voltages. To erase the memory device, negative gate polarity is applied to make the trapped electrons tunnel back to the channel. The control oxide is utilized to prevent the carriers of the gate electrode from injecting into the charge trapping sites by F-N tunneling.

Figure 3 exhibits C-V hysteresis after the bidirectional voltage sweeping. The voltage is swept between 4 and (-7) V or 7 and (-7) V. The erasing voltage is fixed at -7 V. Under the programming voltage of 4 and 7 V, the memory window is 0.1 and 0.93 V, respectively, and increases with the programming voltage. It is worth noting that the hysteresis is counterclockwise which is due to substrate injection from the electrons of the deep inversion layer and holes of the deep accumulation layer of the Si substrate.[11]

Under varied programming voltages and fixed erasing voltage, the relationship between the threshold voltage shift and programming voltage is of special interest. Figure 4 exhibits the gate voltage dependence of the memory window. The threshold voltage shift is increased with the gate voltage. However, two sudden rises of the threshold voltage shift are observed, which take place around 5 and 9.5 V. As the memory device is written with different programming voltages, the tunneling electrons will be captured at the trap states of the Si_3N_4 layer, the interface states between Si_3N_4 and a-Si layers, and/or the quantum well of a-Si. During low-voltage programming, the electrons are captured at the charge-trapping sites of trap states of the Si_3N_4 layer and the interface states between Si_3N_4 and a-Si layers. The sudden rise implies the charge storage of the a-Si quan-
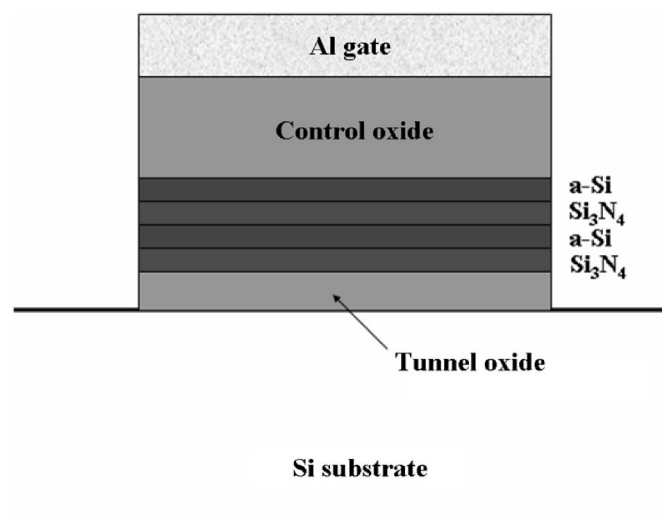
Figure 1. The cross-sectional figure of the quasi-superlattice structure.

Figure 3. C-V hysteresis after the bidirectional voltage sweep. The erasing voltage is fixed at (−7) V.

tum well. Figure 5 shows the programmed band diagram of the memory device. The first sudden rise in Fig. 4 is attributed to the charge storage in the a-Si quantum well between two nitride layers. The second sudden rise is deduced to be that occurring under high-voltage programming when the electrons may be written in to the a-Si quantum well between nitride and control oxide layers. It is also observed that in Fig. 4 the increments of the two sudden rises are obviously different from each other. The increment of the second sudden rise is smaller than that of the first one. The threshold voltage shift is due to the electrons trapped in the gate dielectrics, and the trapped electrons away from the channel influence the threshold voltage less. Therefore, a larger threshold voltage shift is observed among the first low-voltage charge storage in the a-Si quantum well. The threshold voltage of a metal-oxide-semiconductor (MOS) capacitor is described as

$$V_t = V_{FB} + 2\psi_B + \frac{\sqrt{4\epsilon_s q N_A(2\psi_B)}}{C_i} \qquad [1]$$

where V_{FB} is the flatband voltage shift; ϕ_B, the potential difference between the Fermi level, E_F, and the intrinsic Fermi level, E_i; ϵ_s, the permittivity of the semiconductor; N_A, the density of the accep-
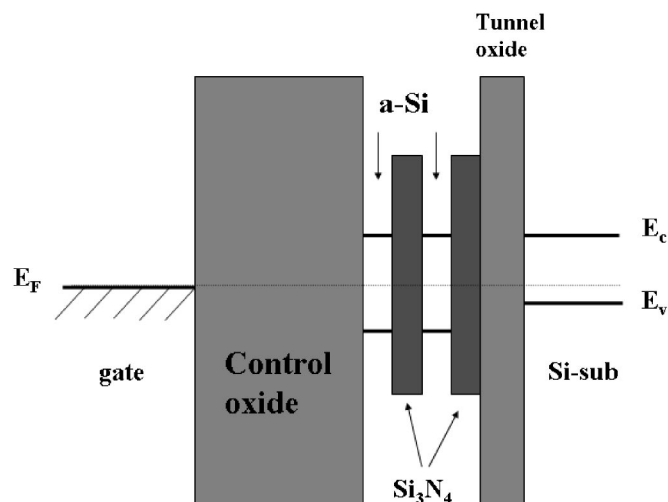
tors; and C_i, the capacitance of the insulator.[12] In this study, the threshold voltage shift, ΔV_t, is mainly determined by the flatband voltage shift, ΔV_{FB}. $\Delta V_t \approx \Delta V_{FB} = Q_t/C_i$, where Q_t is the charge trapped in the quasi-superlattice structure after programming. As inferred in Fig. 4, the trapped charge Q_t is increased with the programming voltage. Under low-voltage programming below 5 V, the injecting charges can tunnel through the tunnel oxide and be trapped in the forbidden gap of the first nitride layer and the interface between Si and Si_3N_4. It is not easy for the electrons to cross
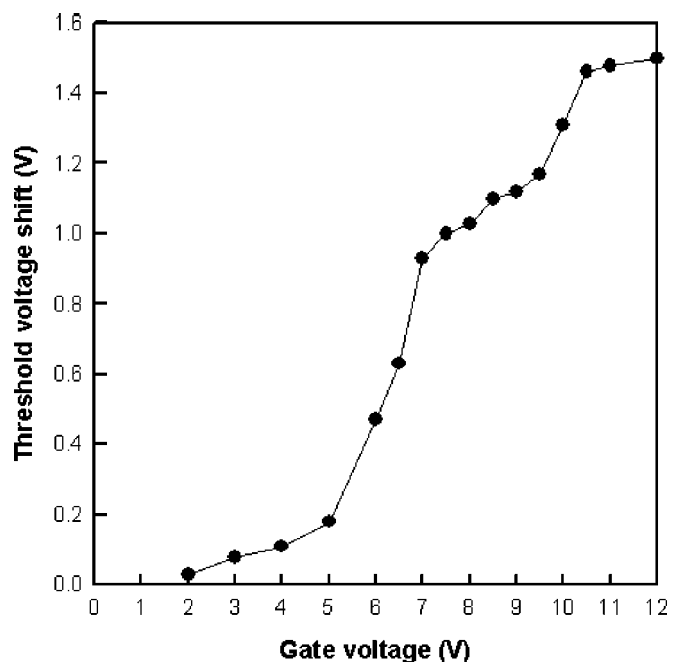

Figure 4. Gate voltage dependence on the memory window. There are two sudden rises of the threshold voltage shift observed, which take place at around 5 and 9.5 V.
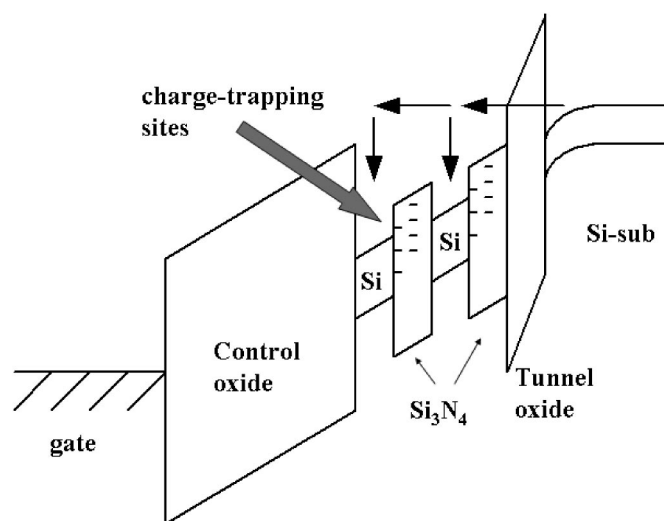

Figure 2. The ideal energy band diagram of the QS² memory device at $V = 0$.

Figure 5. The band diagram of the memory device under programming. Under suitable operating voltages, two apparent states of charge storage can be distinguished.
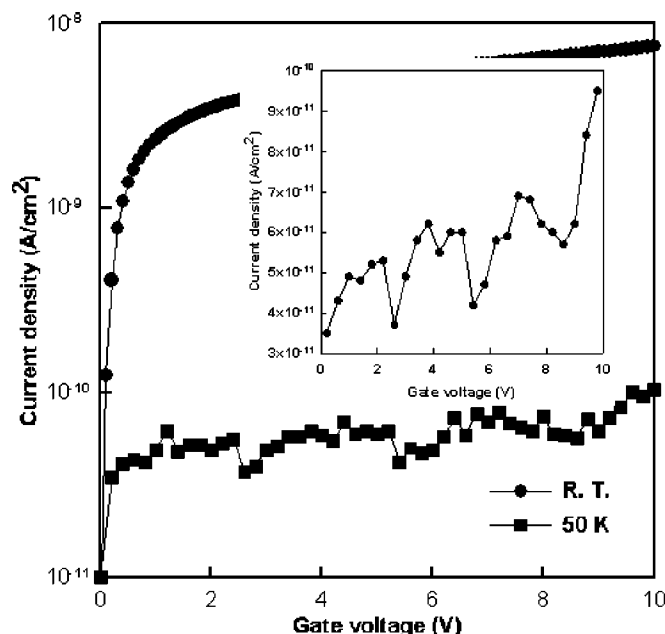

Figure 6. The current *J-V* characteristics for both room temperature and 50 K. The inset shows the local amplification of the *J-V* curve at 50 K.

the barrier height of 3.1 eV between the Si channel and the tunnel oxide via Schottky emission under low-voltage programming. As the programming voltage reaches 5-7 V, the first sudden rise of the threshold voltage shift occurs, which contributes the memory window from 0.2 to 0.93 V. The injecting electrons occupy the energy levels of the Si quantum well during the first sudden rise of the threshold voltage shift. Beyond the programming voltage of 7 V, the increased memory window is attributed to the charge storage in the forbidden gap of the second nitride layer, overcoming the barrier height of ~2.0 eV between Si and the nitride. The programming voltage of 9.5 V and above is needed to lead to the second rise of the threshold voltage shift. In this work, the quasi-superlattice storage implies a 2-bit-per-cell operation by F-N tunneling.[13] In the design of the multilevel storage, bit-1 can be operated in the a-Si quantum well between the nitride layers at a low voltage of about 5-7 V. Bit-2 can be operated in the a-Si quantum well between the nitride and control oxide layers at around 10 V. The 2-bit-per-cell operation is performed by F-N tunneling instead of the conventional channel hot electron injection. Also, the dual read operation of the source side and the drain side for conventional SONOS 2-bit/cell device is not necessary, which simplifies the circuit design engineering.

To investigate the leakage behavior of the quasi-superlattice stack structure, current-voltage electrical measurements are performed. Figure 6 exhibits the current density-voltage (*J-V*) characteristics for both room temperature and at 50 K. It is clearly shown the leakage current at 50 K is lower than that at room temperature by a factor of two orders due to the alleviation of thermionic emission.[14] The leakage current at room temperature, dominated by thermionic emission and trap-assisted tunneling, remains low when 10 V gate voltage is applied. Additionally, there is negative differential resistance observed at different gate biases for the measurements at 50 K. The inset shows the local amplification of the *J-V* curve at 50 K. The negative differential resistance occurs at around 2, 5.2, and 7 V. It is inferred that the current-voltage characteristics behave like those of the resonant tunneling diode (RTD) at low temperature.[15-17] To clarify the similarity between RTD and our quasi-superlattice stack of insulators, a model is proposed based on the energy band diagrams of tunneling. Figure 7 shows the ideal energy band diagram of the quasi-superlattice stack under zero bias with split energy levels. The quasi-superlattice of Si_3N_4 and a-Si clearly shows the band offsets that can easily trap electrons as the memory elements. The undoped a-Si layers have a wider bandgap than those of the Si substrate. In the a-Si quantum wells, discrete energy levels, E_1, E_2,..., and E_n, are formed due to the quantum

confinement effect.[18,19] Consider the resonant tunneling between the two a-Si layers under biases applied. As can be seen in Fig. 8a, after the electrons tunnel from the channel, it is not easy for the electrons to surmount the energy barriers of the nitride and the control oxide at 50 K. Therefore tunneling effects dominate the leakage mechanism. As the applied voltage is around 2 V, the resonant tunneling of E_1 occurs between the two a-Si quantum wells. The first resonant tunneling contributes the peak current density at 2 V as shown in the inset of Fig. 6. As the voltage is applied between 2 and 5.2 V as in Fig. 8b, no energy level exists in the a-Si quantum well for the electrons to resonantly tunnel through. A sudden decrease of the leakage current occurs, followed by the gradual increase of the leakage current, and the second resonant tunneling of E_2 is reached at around 5.2 V. The peak current density at 7 V in Fig. 6 is inferred to be the resonant tunneling of E_3 between the two a-Si quantum wells. During the temperature operation, the leakage behavior is dominated by the tunneling effects which can be described as $J \propto V^2 \exp[-C/V]$, where V is the programming voltage and C is a constant.[20] Considering the quantum confinement of the Si quantum wells, the energy levels are defined as $E_n = n^2\pi^2\hbar^2/2m^*L^2$, where $n = 1,2,3,...,m^*$ is the effective mass of the electrons in the quasi-
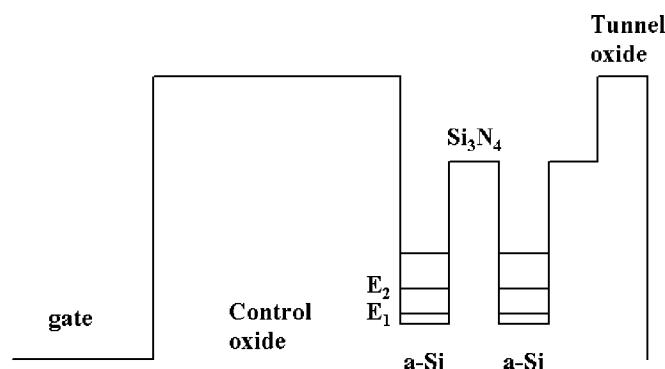

Figure 7. The ideal energy band diagram of the quasi-superlattice stack under zero bias with split energy levels.

(a)

$$V_{applied} \sim 2V$$

E_1

(b)

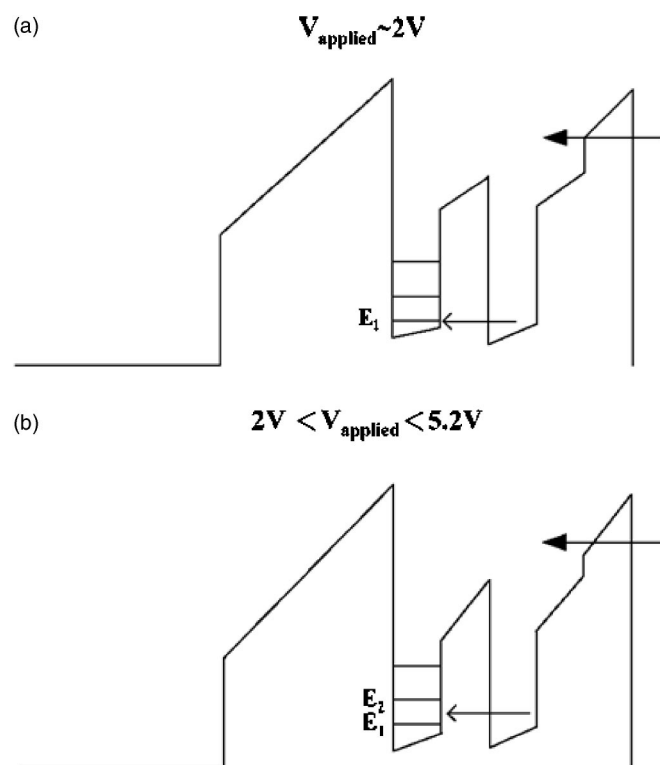$$2V < V_{applied} < 5.2V$$

E_2
E_1

Figure 8. (a) The energy band diagram of resonant tunneling at around 2 V between the two a-Si layers, (b) the band diagram for 2 V < applied gate voltage <5.2 V.

superlattice structure, and *L* is the thickness, ~2 nm, of the Si quantum wells. As $n = 1, 2,$ and 3, $E = E_1, E_2,$ and E_3, the resonant tunneling occurs at the programming voltage of 2, 5.2, and 7 V, respectively. To calculate the resonant voltage drop of the Si quantum wells, m* is estimated to be around 0.19 m_0 for the electrons transported in the Si layer. The first resonant tunneling voltage drop V_{1r} of the Si quantum wells can be calculated by $V_{1r} = 2E_1/q$ = 0.98 V, where $q = 1.6 \times 10^{-19}$ C. Also, V_{2r} and V_{3r} can be calculated as $V_{2r} = 3.92$ V and $V_{3r} = 8.82$ V. The first resonant tunneling is occurres when the programming voltage reached about 2 V. Therefore, the voltage difference of $2 - 0.98 = 1.02$ V is dropped on the tunnel oxide, control oxide, and nitride layers. To motivate the second resonant tunneling, additional voltage is dropped on the Si quantum wells, $V_{2r} - V_{1r}$, needs to be supplied. The additional voltage drop is calculated as 2.94 V, which is close enough to the voltage difference, 3.2 V, of the programming voltage between first and second resonant tunneling. As the programming voltage is increased to 7 V to stimulate the third resonant tunneling, it is deduced that the third resonant tunneling is due to the instability of the two amorphous silicon layers where there should be at least 8.82 V to motivate the third resonant tunneling between the Si quantum wells. The investigation of the leakage mechanism of the quasi-

superlattice stack will help the multilevel charge storage develop the considerations of operating voltage for the 2-bit-per-cell nonvolatile memory device. Further study about the reliability characteristics is being taken into account and is currently under investigation.

Conclusions

In this study, a novel quasi-superlattice storage has been demonstrated for the concept of multilevel charge storage. In the relationship between threshold voltage shift and gate programming voltage, two sudden rises were observed. The obvious memory effects from the measurements of C-V hysteresis exhibited two distinguishable charge storages, which can be utilized as a memory device of 2-bit-per cell. The study on the leakage behavior of the quasi-superlattice stack has also been demonstrated for room temperature and low temperature. The current-voltage characteristics of the quasi-superlattice structure behave like those of the resonant tunneling diode at low temperatures. The negative differential resistance occurs at around 2, 5.2, and 7 V. A concise model is proposed to understand the leakage behavior of the quasi-superlattice stack.

Acknowledgment

References

1. D. Kahng and S. M. Sze, *Bell Syst. Tech. J.,* **46**, 1288 (1967).
2. M. L. Ostraat, J. W. De Blauwe, M. L. Green, L. D. Bell, H. A. Atwater, and R. C. Flagan, *J. Electrochem. Soc.,* **148**, G265 (2001).
3. Z. Liu, C. Lee, V. Narayanan, G. Pei, and E. C. Kan, *IEEE Trans. Electron Devices,* **49**, 1606 (2002).
4. J. J. Welser, S. Tiwari, S. Rishton, K. Y. Lee, and Y. Lee, *IEEE Electron. Devices Lett.,* **18**, 278 (1997).
5. J. D. Blauwe, *IEEE Trans. Nanotechnol.,* **1**, 72 (2002).
6. M. H. White, Y. Yang, A. Purwar, and M. L. French, in *Proceedings of IEEE International Nonvolatile Memory Technology Conference*, 52 (1996).
7. M. H. White, D. A. Adams, and J. Bu, *IEEE Circuits Devices Mag.,* **16**, 22 (2000).
8. D. F. Bentchkowsky, *Proc. IEEE,* **58**, 1207 (1970).
9. B. Eitan, P. Pavan, I. Bloom, E. Aloni, A. Frommer, and D. Finzi, *IEEE Electron. Devices Lett.,* **21**, 543 (2000).
10. H. E. Maes, J. Witters, and G. Groeseneken, in *Proceedings of 17th European Solid State Devices Research Conference, Bologna-1987*, 157 (1988).
11. D. N. Kouvatsos, V. L. Sougleridis, and A. G. Nassiopoulou, *Appl. Phys. Lett.,* **82**, 397 (2003).
12. S. M. Sze, *Physics of Semiconductor Devices*, p. 442, Wiley, New York (1981).
13. W. J. Tsai, N. K. Zous, C. J. Liu, C. C. Liu, C. H. Chen, T. H. Wang, S. Pan, C. Y. Lu, and S. H. Gu, *Tech. Dig. - Int. Electron Devices Meet.,* **2001**, 719.
14. S. M. Sze, *Physics of Semiconductor Devices*, p. 259, Wiley, New York (1981).
15. H. Ikeda, M. Iwasaki, Y. Ishikawa, and M. Tabe, *Appl. Phys. Lett.,* **83**, 1456 (2003).
16. D. J. Paul, P. See, R. Bates, N. Griffin, B. P. Coonan, G. Redmond, G. M. Crean, I. V. Zozoulenko, K. F. Berggren, B. Hollander, and S. Mantl, *Appl. Phys. Lett.,* **78**, 4184 (2001).
17. M. T. Bjork, B. J. Ohlsson, C. Thelander, A. I. Persson, K. Deppert, L. R. Wallenberg, and L. Samuelson, *Appl. Phys. Lett.,* **81**, 4458 (2002).
18. S. R. Sheng, N. L. Rowell, and S. P. McAlister, *Appl. Phys. Lett.,* **83**, 2790 (2003).
19. N. M. Park, S. H. Jeon, H. D. Yang, H. Hwang, S. J. Park, and S. H. Choi, *Appl. Phys. Lett.,* **83**, 1014 (2003).
20. S. M. Sze, *Physics of Semiconductor Devices*, pp. 497-498, Wiley, New York (1981).